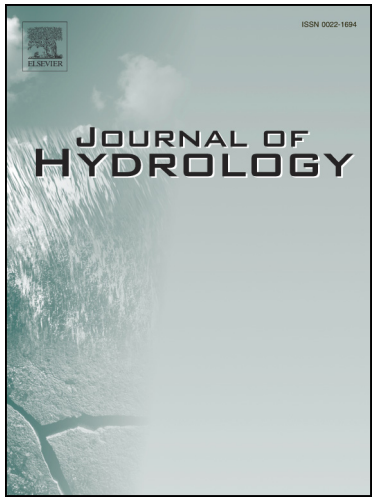

Modelling Sub-daily Latent Heat Fluxes from a Small Reservoir

Ryan McGloin, Hamish McGowan, David McJannet, Stewart Burn

PII: S0022-1694(14)00827-0
DOI: http://dx.doi.org/10.1016/j.jhydrol.2014.10.032
Reference: HYDROL 19982

To appear in: *Journal of Hydrology*

Received Date: 20 February 2014
Revised Date: 15 September 2014
Accepted Date: 11 October 2014

Please cite this article as: McGloin, R., McGowan, H., McJannet, D., Burn, S., Modelling Sub-daily Latent Heat Fluxes from a Small Reservoir, *Journal of Hydrology* (2014), doi: http://dx.doi.org/10.1016/j.jhydrol.2014.10.032

Modelling Sub-daily Latent Heat Fluxes from a Small Reservoir.

Ryan McGloin
Climate Research Group, School of Geography, Planning and Environmental Management, The University of Queensland, Brisbane 4072.
r.mcgloin@uq.edu.au

Hamish McGowan
Climate Research Group, School of Geography, Planning and Environmental Management, The University of Queensland, Brisbane 4072.
h.mcgowan@uq.edu.au

David McJannet
CSIRO Land and Water, 41 Boggo Road, Dutton Park, QLD, 4102.
David.McJannet@csiro.au

Stewart Burn
CSIRO Land and Water, 37 Graham Road, Highett, VIC 3190.
Stewart.Burn@csiro.au

Abstract

Accurate methods of latent heat flux quantification are essential for water management and for use in hydrological and meteorological models. Currently the effect of small lakes in most numerical weather prediction modelling systems is either entirely ignored or crudely parameterized. In order to test methods for modelling hourly latent heat flux from small water bodies, this study compares results from several modelling approaches to values measured by the eddy covariance method at an agricultural reservoir in southeast Queensland, Australia. Mass transfer estimates of *LE* calculated using the theoretical mass transfer model and using the Tanny et al. (2008) and Sacks et al. (1994) bulk transfer coefficients showed the best relationship with measured values under a range of meteorological conditions. The theoretical model showed the strongest correlation with measured values, while the Tanny et al. (2008) and Sacks et al. (1994) models had regression equation slopes with the closest proximity to 1. Latent heat fluxes estimated using the Granger and Hedstrom (2011) evaporation model, that was specifically developed for use at small reservoirs, showed a poor relationship with measured values, particularly in stable atmospheric conditions. The 1-dimensional hydrodynamics model, DYRESM, was used to obtain predictions of hourly latent heat flux without the use of water surface temperature measurements. DYRESM estimates of latent heat flux showed a slightly worse relationship with measured values than those predicted using the traditional mass transfer models (which used measurements of water surface temperature). However, DYRESM performed considerably better than the Granger and Hedstrom (2011) model.

Keywords

Latent heat flux, mass transfer, bulk transfer coefficients, water surface temperature.

1. Introduction

Inland water bodies can vary greatly in spatial scale, from small irrigation reservoirs on farms to large lakes. According to Downing et al. (2006), 50 % of the total global continental surface area covered by water consists of small lakes and reservoirs (<1 km^2). Global estimates of the number of small reservoirs and lakes is in the order of 300 million, with a total surface area of approximately 2.3 million km^2 (approximately 1.5 % of the Earth's continental surface area) (Downing et al., 2006). Despite the large number and importance of small lakes and reservoirs throughout the world, studies of water surface-atmosphere exchanges tend to be biased towards larger bodies of water (Rosenberry et al., 2007). Energy exchanges between the atmosphere and inland water bodies in the form of latent (*LE*) and sensible (*H*) heat fluxes can be ecologically and climatologically important at regional and global scales (Rouse et al., 2005; Long et al., 2007). However, the environmental factors that determine these exchanges, such as wind speed (*u*), humidity and atmospheric turbulence, can be substantially different over small water bodies than over larger lakes (Assouline et al., 2008; Granger and Hedstrom, 2011).

There have been occasional studies that have analysed direct measurements of *LE* from small reservoirs using the state of the art Eddy Covariance (EC) technique (e.g. Tanny et al., 2008, 2011; Nordbo et al., 2011; McGloin et al., 2014a), while other studies have analysed estimates of *LE* derived using the scintillometry method (McJannet et al., 2011, 2013b). Although these methods are essential in understanding the processes controlling *LE*, their use is limited due to the expensive and complex nature of their operation, therefore effective modelling approaches are required. There have been some studies that have evaluated the performance of evaporation models at small reservoirs (i.e. Rosenberry et al., 2007; Tanny et al., 2008; McJannet et al., 2013a). However, most approaches have been limited to

quantifying daily (or greater) estimates of evaporation. Reliable estimates of surface heat fluxes are often necessary to correctly represent the effect that different surface types have on the regional climate (Chen and Dudhia, 2001). In order to accurately model processes such as diurnal variability in Atmospheric Boundary Layer (ABL) height and associated cloud and precipitation processes, it is essential that surface processes are simulated frequently enough to capture the influence the given processes have on the ABL (i.e. time-steps in the order of one hour) (Chen and Dudhia, 2001; Pielke, 2001; Pitman, 2003).

Understanding the relationship between small lakes and the local climate is of particular interest for regions where there is a high density of such lakes (e.g., in permafrost, periglacial, and riverine landscapes) (MacKay et al., 2009). In these environments small water bodies can represent up to 10 % of the local land surface area (MacKay et al., 2009; Nordbo et al., 2011; Bouin et al., 2012). Although few studies have focused specifically on analysing the impact of small lakes on regional climates, authors such as MacKay et al. (2009), Balsamo et al. (2012) and Martynov et al. (2012) have indicated the potential importance of these water bodies in modifying the local climates of regions where they are abundant. Currently, the effect of small to medium size lakes in most numerical weather prediction (NWP) and climate modelling systems is either entirely ignored or crudely parameterized (Mironov et al., 2010). However, with continuing improvements in the horizontal resolution of NWP systems such as the Weather Research and Forecasting model (WRF), it is likely that in the near future there will be the potential to effectively model the effects of small lakes on regional weather. However, this will require accurate parameterisations of water surface-atmosphere exchanges at sub-daily timesteps.

In this study three models were selected according to their potential to accurately model sub-daily estimates of *LE* from a small reservoir. Model selection was limited by the need to use sub-daily inputs. For example, widely used methods like the energy balance or combination methods (such as the Priestly-Taylor (Priestly and Taylor, 1972) and Penman-Monteith (Monteith, 1965) methods) were not considered for use in this study because they require an estimate of the change in water body heat storage, which is notoriously difficult to quantify accurately at short time-steps. In addition, in order to allow researchers to replicate this study's methodology in locations where available input data may be limited, it was decided to keep model complexity to a minimum.

Each of the selected modelling techniques used in this study are based on the mass transfer model principle, where *LE* is determined as a function of u and the difference in humidity between the water surface and overlying air (Stull, 1988). The first of the selected modelling techniques in this study is the traditional mass transfer model, which simply determines *LE* using the $u(q_s - q_a)$ function (where $(q_s - q_a)$ is the difference between the specific humidities of the water surface and air) and a bulk transfer coefficient (C_E). The second technique is a model developed by Granger and Hedstrom (2011) for the specific purpose of estimating sub-daily evaporation from small reservoirs. Both the traditional mass transfer and Granger and Hedstrom (2011) models require site-specific meteorological measurements and measurements of water surface temperature (T_s). However, in many cases over-water meteorological measurements and T_s measurements are unlikely to be available. Therefore, the third model tested was the one-dimensional hydrodynamics model known as DYRESM (Dynamic Reservoir Simulation Model) (Imberger and Patterson, 1981; Imerito, 2010a), which does not require user specification of T_s. DYRESM is used to predict the vertical distribution of temperature in water bodies at daily and sub-daily time-steps. It has been used

at a wide variety of water bodies with different morphologies and climates (e.g. Gal et al., 2003; Perroud et al., 2009; Weinberger and Vetter, 2012). However, most applications of the model have been related to water body ecology or water quality rather than for the specific purpose of *LE* quantification.

This study explores the potential to accurately model *LE* at hourly time steps from a small agricultural reservoir in southeast Queensland, Australia. Latent heat flux predictions made by the traditional mass transfer, Granger and Hedstrom (2011) and DYRESM models are assessed through comparison with measurements made on site using an EC system. Explanations for differences between measured and modelled results are provided and periods where model performance varied with changes in the ambient meteorological conditions are identified.

2. Methods

2.1 Study Site

Field measurements were conducted at Logan's Dam (27°34'25.93"S; 152°20'27.45"E; altitude 88 m), located approximately 75 km west of Brisbane in southeast Queensland, Australia. Note that "Logan's Dam" refers to the water storage reservoir used in this study (in Australia it is common to refer to man-made reservoirs as "dams"). The reservoir wall is constructed of compacted earth and is roughly rectangular in shape with dimensions of approximately 480 m × 350 m. The reservoir has an approximate surface area of 0.17 km^2, a storage capacity of 0.7 GL and a maximum depth of 6 m. The terrain surrounding Logan's Dam is complex with the water body, forested areas (to the north, south and west), the reservoir wall and farm land all within a short distance of one another. For an image of Logan's Dam and the location of some of the equipment described in the following sections

see Figure 1 in McGloin et al. (2014a). Note that previous micrometeorological studies at Logan's Dam (i.e. McJannet et al., 2011; McJannet et al., 2013a; McJannet et al., 2013b; McGloin et al., 2014a; McGloin et al., 2014b) focused on analysing surface heat flux measurements and did not present any analysis involving methods for modelling sub-daily *LE*.

A 47-year time series (1965-2011) of archived meteorological data from the nearest available Bureau of Meteorology (BOM) weather station (Gatton 040082), located approximately 3 km north of Logan's Dam, was used to provide a long-term summary of the climatic conditions in the region. The mean maximum and minimum air temperatures (T_a), vapour pressure (e_a) and u over the 47 year record were 26.8 °C, 13.2 °C, 1.64 kPa and 2.74 m s^{-1}, respectively, while the mean annual rainfall was 781 mm. The region experiences a seasonal subtropical climate (Bureau of Meteorology, 2005) with the warmest and wettest weather during summer and the coolest and driest weather in winter. Two types of meteorological conditions characterise the climate of the study site. Moist easterly winds dominate for the majority of the year (especially in summer) and comparatively dry westerly winds dominate in winter, with transitional periods between.

2.2 Equipment and Measurements

2.2.1 Eddy Covariance

The EC technique involves determination of surface heat fluxes using high frequency measurements of vertical wind velocity by a sonic anemometer and the density of scalars by an infrared gas analyser. For this study a full year of EC data, from 1 March 2010 to 28 February 2011, was selected for analysis. The EC system setup included a sonic anemometer (CSAT-3, Campbell Scientific, Utah, USA) installed at a height of 2.4 m, an open-path H_2O

and CO_2 infrared gas analyser (CS7500, LiCor, Lincoln, USA) installed at a height of 2.4 m and a net radiometer (CNR1, Kipp & Zonen, Delft, Netherlands) installed at a height of 1.4 m. The EC unit was located on a pontoon near the centre of the reservoir and supplied with power from mounted solar panels. The pontoon consisted of a square platform that had an approximate surface area of 2.5 m × 2.5 m, the platform was kept a float by four large drums and was held in position by 4 mooring lines.

The EC unit was controlled by a CR3000 data logger (Campbell Scientific, Utah, USA) with measurements of *LE* (W m^{-2}) and *H* (W m^{-2}) calculated using 15-minute covariances of the turbulent components of vertical wind velocity (w'), water vapour density (ρ_w') and air temperature (T_a'). For analysis in this study, hourly averages of the 15-minute values were used. Tilt error (Lee et al., 2005), frequency response (Massman, 2000) and Webb-Pearman-Leuning (Webb et al., 1980) flux corrections were then performed in post-processing. All EC data recorded during rain events and obvious outliers were removed. Note that gaps in the EC *LE* measurements were not filled in this study. For more on the EC flux calculation, correction and quality control procedures used in this study see McGloin et al. (2014a). A detailed analysis of EC measurement footprints in McGloin et al. (2014a) suggested that in the majority of conditions the EC footprint was located within the reservoir boundaries. For example, cumulative footprints for southeasterly and westerly winds (most frequent wind directions), showed that the percentages of footprint originating from the reservoir surface during neutral atmospheric conditions were 92 % (SE) and 95 % (W), respectively.

The short fetch of Logan's Dam generally resulted in very small waves and very little pontoon motion. The wave conditions were significantly different from those typically observed at sea or large lakes, where extensive corrections for platform motion are

recommended (Edson et al., 1998). Using the same pontoon and instrument configuration as this study to quantify surface energy exchanges over a coral reef, Wiebe et al. (2011) concluded that although wave induced motion was visible in the wind velocity spectra, the oscillation did not strongly influence the co-spectrum of the flux measurements. In addition, using a very similar instrumental set up, Eugster et al. (2003) concluded that there was no need for a special flux correction to eliminate traces of pontoon oscillation at a small reservoir similar to Logan's Dam.

2.2.2 Floating and Land-Based Weather Stations

A separate floating weather station platform was positioned in a central location on the reservoir (note that from now on this weather station is referred to as the floating weather station). Equipment on the platform included a net radiometer (CNR1, Kipp & Zonen, Delft, The Netherlands) installed at a height of 1.2 m, an anemometer (014A, MetOne, Oregon, USA) installed at a height of 2.4 m and a temperature and humidity sensor (CS215, Campbell Scientific, Utah, USA) installed at a height of 2.5 m. The net radiometer provided measurements of net radiation (R_n) (W m^{-2}) and estimates of water surface skin temperature (T_{skin}) (°C), while the anemometer provided measurements of u (m s^{-1}) and the temperature and humidity sensor provided measurements of T_a (°C) and e_a (kPa), respectively. Note that T_{skin} values were calculated using net radiometer measurements of upwelling long-wave radiation. Measurements of the temperature profile in the reservoir were given by a thermistor chain (Precision Measurement Engineering, California, USA) suspended below the floating platform, with water temperature measurements made at 0.3 m increments from 0.1 m to 4.3 m deep (note that only the measurements at 0.1 m deep were used in this study). Weather stations were also positioned on each of the four reservoir walls, with each station consisting of a tipping bucket rain gauge (TB3, Hydrological Services, Sydney, Australia), a

2D Windsonic installed at a height of 2 m (Gill, Hampshire, England) and a CS215 temperature and humidity sensor (Campbell Scientific, Utah, USA) installed at a height of 2 m.

2.2.3 Pumped Inflows and Outflows

Refilling of Logan's Dam occurred through two large 800 mm diameter pipes. Two distribution pipes, one with a diameter of 200 mm and the other with a diameter of 250 mm, were used for withdrawing water to irrigate crops. The distribution pipes were fitted with high accuracy (±0.2%) flow meters (Magflow Mag5100W, Siemens, Victoria, Australia) and transmitters (Mag6000, Siemens, Victoria, Australia) to determine total outflow. Only the commencement and cessation of pumped inflow events were recorded because of potential errors associated with measuring the large volumes of water that flowed through the inflow pipes. Between March 2010 and February 2011 there were just two occasions when water was pumped into the reservoir (lasting a combined total of 14 days), while withdrawal events were reasonably frequent.

2.3 Evaporation Models

2.3.1 Traditional Mass Transfer

Evaporation from a water surface can be calculated using the traditional mass transfer model given by:

$$E = C_E \rho u (q_s - q_a) \quad (1)$$

where E is evaporation (kg m^{-2} s^{-1}), ρ is air density (kg m^{-3}) and q_s and q_a are the specific humidities (kg kg^{-1}) of the water surface and air, respectively. Note that E values were converted to LE (W m^{-2}). In order to account for the effects of surface roughness and atmospheric stability, equation 1 also requires a bulk transfer coefficient, C_E. An approximate

constant site-specific C_E value can be derived empirically by plotting EC measurements of *LE* against $\rho u(q_s - q_a)$ and then forcing the regression line through the origin. Site-specific C_E values can also be estimated as a function of *u* using direct measurements of *u*, *LE* and $(q_s - q_a)$, as outlined in Tanny et al (2008).

Since most researchers will not have access to EC measurements of *LE*, we decided to test traditional mass transfer methods that are completely independent of EC measurements. One approach is to use an empirically-derived constant site-specific C_E value from a previous study. A problem with this approach is that there is a lot of variation in the C_E values from different studies; hence it is not always obvious which value is most appropriate for a particular field site. Therefore, a range of C_E values from studies over open-water are compared in this study (see Table 1). Note that it is standard practice to express C_E for a measurement height of 10 m (Sene et al., 1991). Therefore, Table 1 shows C_E values for the measurement heights given in each study and after they have been adjusted using the logarithmic wind profile formula for a measurement height of 10 m.

Table 1: Bulk transfer coefficients that are tested in this study.

Study	C_E	Measurement height (m)	C_E (adjusted for a measurement height of 10 m)	Site
Brutsaert (1982) (is also the value used in the DYRESM model (see section 2.3.3))	1.30×10^{-3}	10.0	1.30×10^{-3}	Various oceans and lakes
Sacks et al. (1994)	1.88×10^{-3}	2.0	1.62×10^{-3}	Lake Barco, Florida, USA (0.11 km^2)
Rosenberry et al. (2007)	1.64×10^{-3}	2.0	1.41×10^{-3}	Mirror Lake, New Hampshire, USA (0.15 km^2)
Tanny et al. (2008)	1.88×10^{-3}	2.9	1.67×10^{-3}	Eshkol reservoir, north Israel (1 km^2)

Bulk transfer coefficients can also be estimated theoretically using the approach described in Brutsaert (1982), where C_E is defined as:

$$C_E = \frac{k^2 Cd^2}{\ln(\frac{z}{z_{0v}}) - \psi_{sv}(\frac{z}{L})} \quad (2)$$

where z is the measurement height (2.4 m), k is the Von Karman constant (0.41), z_{0v} is the scalar roughness length (m), $\psi_{sv}(\frac{z}{L})$ is the universal stability function for water vapour and Cd is the drag coefficient. The universal stability function for water vapour was calculated using the relationships for stable and unstable conditions described in Brutsaert (1982). Note that to keep model results independent of EC measurements, the stability of the atmosphere was assessed in this study using the Bulk Richardson number (Stull, 1988):

$$R_B = \frac{g\Delta T z}{Tu^2} \quad (3)$$

where ΔT (K) is the difference in temperature between the water surface and instrumentation and g/T is the buoyancy parameter. The Bulk Richardson numbers were then converted into stability parameter (z/L) values using the formula proposed by Andreas and Murphy (1986).

The expression of z_{0v} for a smooth water surface is given by equation 4 (Brutsaert, 1982):

$$z_{0v} = 0.624\frac{v}{u_*} \quad (4)$$

where u_* is the friction velocity (m s^{-1}) and v the kinematic viscosity of air (m^2 s^{-1}). Equation 5 defines Cd for open-water surfaces (Brutsaert, 1982):

$$Cd = \frac{k^2}{(\ln(\frac{z}{z_{0m}}) - \psi_m(\frac{z}{L}))^2} \quad (5)$$

where z_{0m} is the momentum roughness length (m) and $\psi_m(\frac{z}{L})$ is the universal stability function for momentum. The universal stability function for momentum was calculated using the relationships for stable and unstable conditions described in Paulson (1970).

Friction velocity values for open-water were calculated in this study using the following equation (Stull, 1988):

$$u_* = \frac{uk}{\ln(\frac{z}{z_{0m}}) - \psi_m(\frac{z}{L})} \tag{6}$$

where the value for z_{0m} was derived using the Zilitinkevich (1969) equation for estimating z_{0m} over open-water:

$$z_{0m} = c_1 \frac{v}{u_*} + \frac{u_*^2}{g c_2} \tag{7}$$

where g is the gravitational constant, c_1 is 0.48 and c_2 is 81.1. An initial u_* value was calculated using a roughness length value of 0.0001 m, this value was then substituted into equation 7 and the resulting solution was fed back into equation 6. This iterative procedure was continued until a stable solution for z_{0m} was obtained.

2.3.2 Granger and Hedstrom

Granger and Hedstrom (2011) presented a simple model for estimating hourly *LE* from small lakes:

$$LE = au \tag{8}$$

where

$$a = b + m(T_a - T_s) + n(e_s - e_a) \tag{9}$$

Parameters include u (m s^{-1}), vapour pressure difference between the water surface and air, e_s-e_a (kPa), and temperature difference, T_a-T_s (°C). Note that Granger and Hedstrom (2011) found that LE was substantially suppressed when conditions were stable ($T_a > T_s$) and enhanced when conditions were unstable ($T_a < T_s$). The coefficients b, m and n are given by

$$\begin{aligned} b &= 3.395 + 0.0008X \\ m &= -4.584 + 0.420\ln(X) \\ n &= 20.256 - 0.0011X \end{aligned} \quad (10)$$

in stable conditions, and

$$\begin{aligned} b &= 2.373 + 0.0002X \\ m &= -1.758 + 0.0904\ln(X) \\ n &= 26.525 - 0.0008X \end{aligned} \quad (11)$$

in unstable conditions, where X (m) is the upwind fetch (distance from upwind shore).

2.3.3 DYRESM

DYRESM (v4.0) was developed by the Centre for Water Research at the University of Western Australia, to predict the vertical distribution of temperature, salinity and density in lakes and reservoirs (Imberger and Patterson, 1981; Imerito, 2010a). The model is based on the Lagrangian layer scheme, where the lake is modelled by a series of uniform horizontal layers. Layer thickness changes as layers combine, expand, contract, divide and move up and down as they are affected by the physical processes represented in the model (Imerito, 2010a; Etemad-Shahidi et al., 2010). Layer mixing occurs when the turbulent kinetic energy in the topmost horizontal layer exceeds a potential energy threshold. The kinetic energy is produced by convection, wind stirring and shearing (Imerito, 2010a). A fundamental assumption of DYRESM is that horizontal variations in lake density are weak and that the restoring force of stratification is greater than the disturbing force of the wind (Imerito, 2010a).

As input data, DYRESM requires the lake geometry, daily or sub-daily meteorological data, daily inflows (m^3 d^{-1}) (and inflow water temperature), daily outflows (m^3 d^{-1}), an initial water temperature profile (from which DYRESM obtains the initial water depth) and the light extinction coefficient (=1.0 in this analysis). The data requirements are described in detail in Imerito (2010b). Required meteorological data consists of u (m s^{-1}), e_a (hPa), T_a (°C), incident short-wave radiation (W m^{-2}), rainfall (mm) and either the net long-wave radiation (W m^{-2}), incident long-wave radiation (W m^{-2}) or fraction of cloud cover (value ranging from 0 to 1). In order to accurately predict water temperatures, DYRESM needs to account for surface cooling caused by evaporation. Therefore, DYRESM uses the water temperature in the uppermost water layer and equation 1 (with a fixed C_E value of 1.3×10^{-3} for a measurement height of 10 m) to estimate *LE* at each time-step.

2.4 Model Sources of Data

Model estimates of *LE* were calculated at hourly time-steps between 1 March 2010 and 28 February 2011. Measurements for the traditional mass transfer models consisted of measurements of u and q_a taken from the floating weather station, while q_s values were calculated using T_{skin} estimates from the net radiometer on the floating weather station. Note that for the purposes of this study "traditional mass transfer model" refers to any model that calculates *LE* values using equation 1 and T_{skin} estimates from the net radiometer. All of the measurements required to perform the stability corrections and to estimate z_{0m} and u_* for the theoretical mass transfer model, were also taken from the floating weather station. For the mass transfer calculations made using each of the bulk transfer coefficients listed in Table 1, u values measured at a height of 2.4 m on the floating weather station were converted to a height of 10 m using the logarithmic wind profile formula.

The Granger and Hedstrom (2011) model requires over-land measurements of T_a and e_a and over-water measurements of T_s, e_s and u (at a height of 2 m). Measurements of u made at the floating weather station were converted to a height of 2 m using the logarithmic wind profile formula, while T_{skin} values from the floating weather station were used to represent T_s (from which e_s values were calculated). Over-land meteorological measurements were taken from the weather stations positioned on the reservoir walls. In order to obtain the upwind over-land meteorological conditions the weather station data selected was dependent on the wind direction. During easterly winds (0-180°) over-land measurements of T_a and e_a were taken from the easterly weather station at a height of 2 m, while during westerly winds over-land measurements of T_a and e_a were taken from the westerly weather station. Note that X values of 220 m and 224 m were used to represent the distance from the floating weather station to the upwind edge of the reservoir during easterly and westerly winds.

As DYRESM does not require T_s specification it provides an opportunity to run the model in two modes which reflect the potential availability of data at a given site. The first mode represents a highly instrumented site, where all the required variables are measured directly, while the second represents the more commonly experienced data sparse environment, where nearby meteorological measurements made over land are all that is available. For the highly instrumented scenario u, T_a, and e_a values were all taken from the floating weather station, while upwind land-based weather station measurements were used for the data limited scenario. Both scenarios used incident short-wave radiation from the floating net radiometer. The incident long-wave radiation was also taken from the net radiometer for the highly instrumented scenario, while for the data limited scenario incident long-wave radiation was estimated using the methodology presented by Sridhar and Elliott (2002).

A bathymetric survey of Logan's Dam was undertaken by G.L. Irrigation Pty Ltd. using a dual frequency GPS (NovAtel RTK, NovAtel Inc., Alberta, Canada) (note that this survey was performed immediately after the reservoir was constructed and before it was filled). The bathymetry data was used to estimate the reservoir geometry for the highly instrumented scenario. For the data limited scenario, the reservoir was assumed to be a box with dimensions of 480 m × 350 m × 6.0 m. For the highly instrumented scenario, daily outflow volumes were taken from the flow meters positioned on each of the outflow pipes, while the model was stopped during each of the inflow events and restarted with updated water profile data. For the data limited scenario, daily outflows were assumed to be equal to the average daily volume of water pumped out of Logan's Dam (approximately 850 ML), while it was assumed that the reservoir was initially filled to capacity but with no further inflows during the year. Measured initial temperature profiles were used for the highly instrumented scenario. For the data limited scenario T_a was used as the initial water temperature at all depths within the reservoir. This required the model to run for a spin-up period until the influence of the initial temperature profile was no longer observed in the model output. Therefore, for the data limited scenario, DYRESM was run for a spin-up period of one month (February 2010). Table 2 summarises the sources of data for the DYRESM highly instrumented and data limited scenarios.

Table 2: Sources of data for DYRESM scenarios.

Method	Meteorological data	Reservoir geometry	Inflows/outflows	Initial profile
Highly instrumented scenario	Over-water measurements. Incident short-wave and long-wave radiation data taken from net radiometer.	Bathymetric survey data.	Model stopped during inflows. Direct measurements of outflows.	Measured
Data limited scenario	Over-land measurements. Incident shortwave radiation data taken from net radiometer. Modelled incident long-wave radiation.	Assumed to have box dimensions.	Constant outflow rate. No inflows.	Air temperature used as the initial water temperature at all depths. Model spin-up period of one month.

3. Results

3.1 Model Comparisons with Measurements

Model performance was tested by performing regression analysis between EC measurements of hourly *LE* and values from the various modelling techniques (Table 3). The regression equation for theoretical mass transfer *LE* values against EC *LE* values had a slope that was less than 1, indicating that the model tended to underestimate *LE*. However, the correlation (R^2) between theoretical mass transfer *LE* values and measured *LE* values was the strongest of the models tested and the theoretical mass transfer model also had the lowest Root Mean Square Error (RMSE) (Figure 1a and Table 3).

Table 3: Summary of regression analysis comparing *LE* measurements with values predicted by the various modelling techniques. Note that all p-values for the regression analysis were ≈ 0.00.

Method	R^2	slope	y-intercept	RMSE (W m^{-2})
Theoretical mass transfer	0.86	0.74	7.11	26.44
Brutsaert (1982) mass transfer	0.83	0.79	-3.65	31.87
Sacks et al. (1994) mass transfer	0.83	0.98	-4.54	26.65
Rosenberry et al. (2007) mass transfer	0.83	0.85	-3.96	28.77
Tanny et al. (2008) mass transfer	0.83	1.02	-4.71	27.10
Granger and Hedstrom (2011)	0.59	0.48	5.98	51.26
Highly instrumented DYRESM scenario	0.78	1.07	2.81	34.19
Data limited DYRESM scenario	0.70	1.07	3.04	42.18

Latent heat flux values modelled using the various constant site-specific C_E values listed in Table 1 showed slightly worse correlations with EC values than the theoretical mass transfer model. This is most likely related to the influence of atmospheric stability and variable roughness length, which are accounted for in the theoretical model but not in the other traditional mass transfer methods. The slopes of the regression equations for the Tanny et al. (2008) and Sacks et al. (1994) mass transfer models showed the closest proximity to 1 of all the models tested (Figure 1b and Table 3). In addition, both the Tanny et al. (2008) and Sacks et al. (1994) models had RMSE values that were only slightly greater than the value for the theoretical mass transfer model. The Rosenberry et al. (2007) and Brutsaert (1982) mass transfer models model had regression equation slopes that were less than 1, while the models ranked fourth and fifth in terms of RMSE value, respectively.

Latent heat fluxes modelled using Granger and Hedstrom's (2011) model showed a poor relationship with measured values. The slope of the regression equation for the Granger and Hedstrom (2011) model was much less than 1, while it had the lowest R^2 value and the highest RMSE value of the models tested in this study. The regression equations for both DYRESM scenarios were very similar, with the slopes of the equations showing a reasonably close proximity to 1, while the R^2 values were lower than the values found for the traditional mass transfer models. As expected the *LE* estimates of the highly instrumented scenario showed a stronger correlation with measured results and had a lower RMSE value than *LE* values estimated using the data limited scenario. The RMSE values for the highly instrumented and data limited scenarios were the sixth and seventh lowest of the models tested, respectively.

3.2 Variations in Model Performance

In this section diurnal variations in model performance are analysed (Figure 2a and Table 4). Mean theoretical mass transfer *LE* values were constantly less than mean EC values, with greatest differences in the early afternoon when EC *LE* typically reached its peak (Figure 2a). Mean Granger and Hedstrom (2011) *LE* values were also constantly less than mean EC values, with very large differences observed during the middle of the day. Best agreement (highest R^2 and lowest RMSE) between EC *LE* measurements and Granger and Hedstrom (2011) estimates occurred during night-time (1800-0600) (Table 4). Mean Tanny et al. (2008) mass transfer *LE* results were less than mean EC values during the majority of the day and night, with periods of greater modelled *LE* during the afternoon (Figure 2a and Table 4). Mean DYRESM *LE* values were predominantly greater than mean EC values, with the exception of the late morning (0600-1200), when modelled *LE* tended to be slightly less. The

worst relationship between EC *LE* measurements and DYRESM estimates was observed during the late afternoon/early evening (1500-1800) (Figure 2a and Table 4).

Seasonal variations in model performance were also analysed (Figure 2b and Table 5). Differences between mean EC *LE* measurements and theoretical mass transfer *LE* estimates were greatest in summer; however this was most likely because of the greater magnitude of *LE* in summer. The regression equations and R^2 values for EC *LE* measurements against theoretical mass transfer estimates were similar in each season (Table 5). In contrast, there was a particularly poor agreement between hourly EC *LE* measurements and Granger and Hedstrom (2011) estimates during winter (very low R^2 and high RMSE) (Table 5). Tanny et al. (2008) *LE* mass transfer estimates tended to be greater than EC values during winter and less than EC values during summer (Figure 2b and Table 5). Mean DYRESM *LE* values calculated using the highly instrumented and data limited scenarios were greater than EC measurements in every season except spring, when data limited DYRESM scenario estimates tended to be slightly less than measured values. Greatest differences between DYRESM *LE* estimates and measured values occurred in autumn (Figure 2b).

Table 4: Summary of regression analysis comparing EC *LE* measurements with values predicted by the various modelling techniques during specific 6-hour time blocks. Note that all p-values for the regression analysis were ≈ 0.00.

Method	0000 - 0600				0600 - 1200				1200 - 1800				1800 - 0000			
	R^2	Slope	y-intercept	RMSE (W m^{-2})	R^2	Slope	y-intercept	RMSE (W m^{-2})	R^2	Slope	y-intercept	RMSE (W m^{-2})	R^2	Slope	y-intercept	RMSE (W m^{-2})
Theoretical mass transfer	0.80	0.63	13.86	20.35	0.88	0.73	6.72	27.93	0.85	0.80	1.05	33.25	0.81	0.71	10.29	20.87
Tanny et al. (2008) mass transfer	0.80	0.79	-0.93	21.56	0.85	1.01	-9.43	25.71	0.78	0.99	14.76	35.85	0.76	0.86	1.70	22.60
Granger and Hedstrom (2011)	0.77	0.70	5.74	22.06	0.69	0.49	-1.78	59.01	0.61	0.51	-6.04	74.47	0.76	0.69	4.69	26.22
Highly instrumented DYRESM scenario	0.83	1.02	6.04	20.04	0.81	1.12	-12.61	32.05	0.69	1.03	17.09	49.40	0.77	1.03	7.02	25.29
Data limited DYRESM scenario	0.64	0.96	9.45	30.39	0.72	1.08	-12.27	38.91	0.60	1.03	17.08	58.15	0.74	1.21	-0.05	34.47

Table 5: Summary of regression analysis comparing EC *LE* measurements with values predicted by the various modelling techniques in each season. Note that all p-values for the regression analysis were ≈ 0.00.

Method	Autumn				Winter				Spring				Summer			
	R^2	Slope	y-intercept	RMSE (W m^{-2})	R^2	Slope	y-intercept	RMSE (W m^{-2})	R^2	Slope	y-intercept	RMSE (W m^{-2})	R^2	Slope	y-intercept	RMSE (W m^{-2})
Theoretical mass transfer	0.85	0.74	12.45	21.13	0.86	0.80	4.03	16.85	0.90	0.76	5.48	23.70	0.86	0.75	2.10	36.33
Tanny et al. (2008) mass transfer	0.83	1.11	-4.72	25.74	0.85	1.20	-5.10	22.91	0.86	1.05	-7.90	24.54	0.84	1.02	-19.05	33.42
Granger and Hedstrom (2011)	0.56	0.43	14.48	42.80	0.06	0.19	17.16	52.85	0.74	0.56	2.77	44.26	0.68	0.50	2.90	65.60
Highly instrumented DYRESM scenario	0.76	1.13	4.73	35.42	0.83	1.19	-2.52	24.56	0.80	1.08	-0.43	31.50	0.76	1.05	1.01	39.80
Data limited DYRESM scenario	0.74	1.19	5.44	41.20	0.62	1.00	8.71	32.95	0.69	0.97	2.18	36.56	0.69	1.14	-6.25	52.91

3.3 Bulk Transfer Coefficient Analysis

Plotting EC *LE* measurements against $\rho u(q_s - q_a)$ and then forcing the regression line through the origin gives an approximate constant C_E value that is specific to Logan's Dam of 2.00×10^{-3} (for a measurement height of 2.4 m). Adjusting this value for a measurement height of 10 m gives a C_E value of 1.76×10^{-3}. Typically, turbulent exchanges of *LE* are promoted during unstable conditions ($T_s > T_a$) and suppressed during stable conditions ($T_a > T_s$). Repeating the analysis above for unstable and stable atmospheric conditions resulted in constant C_E values (for a measurement height of 10 m) of 2.07×10^{-3} for unstable conditions and 1.50×10^{-3} for stable conditions, respectively.

Site-specific C_E values can also be estimated empirically using a wind function derived from direct measurements of *LE, u* and $(q_s - q_a)$, as outlined in Tanny et al (2008). The resulting empirical wind function for Logan's Dam was $C_E = 1.5\times10^{-3} + 1.6\times10^{-3}/u$. Figure 3 shows the relationship between C_E values calculated theoretically and those calculated using the empirical wind function. Best agreement between theoretically and empirically derived C_E values occurred in low wind speeds (in unstable atmospheric conditions), while theoretical C_E values were underestimated in moderate-high wind speeds (>2 m s^{-1}) (in stable and neutral atmospheric conditions) (Figure 3). It is clear that for wind speeds below 3 m s^{-1}, C_E tended to decrease with increasing *u*, while for wind speeds above 3 m s^{-1}, C_E showed little dependence on *u*. Other studies such as Ikebuchi et al. (1988), Sene et al. (1991) and Tanny et al. (2008) have made similar observations.

3.4 Water Surface Temperature Analysis

As noted earlier one of the key differences between DYRESM and the other models used is that water temperature does not need to be specified. However, this means that the model

needs to predict T_s accurately to produce reliable *LE* estimates. Comparisons were made between thermistor chain measurements of water temperature at a depth of 0.1 m ($T_{0.1m}$), T_{skin} estimates from the CNR1 sensor on the floating weather station and DYRESM T_s estimates (temperature in uppermost water layer) for the highly instrumented and data limited scenarios (Figure 4). The data limited DYRESM scenario tended to overestimate T_s, while results from the highly instrumented scenario generally showed a very strong relationship with $T_{0.1m}$ measurements. Regression analysis between hourly $T_{0.1m}$ measurements and T_s values predicted by the highly instrumented and data limited DYRESM scenarios for the entire measurement period, resulted in the following equations; $T_{sDYRESM}=1.10T_{0.1m}-2.15$, $R^2=0.97$ with RMSE=0.97 °C and $T_{sDYRESM}=1.15T_{0.1m}-2.20$, $R^2=0.96$ with RMSE=1.68 °C. Estimates of T_{skin} were substantially lower than $T_{0.1m}$ measurements and DYRESM T_s estimates during the majority of the day, particularly at night-time (Figure 4). Best agreement between T_{skin} and $T_{0.1m}$ occurred during the late morning/early afternoon (0900-1500). The regression equation for hourly $T_{0.1m}$ measurements against T_{skin} values for the entire measurement period was; $T_{0.1m}=0.87T_{skin}+4.15$, $R^2=0.93$ with RMSE=2.11 °C.

4. Discussion

A strong correlation was found between EC *LE* measurements and traditional mass transfer predictions, this was the result of the very strong relationship between *LE* and $u(e_s-e_a)$ at Logan's Dam (see McGloin et al., 2014a). Studies at a variety of other water bodies (e.g. Sene et al., 1991; Blanken et al., 2000; Blanken et al., 2003; Nordbo et al., 2011) have not reported such a strong relationship between *LE* and $u(e_s-e_a)$. In section 3.3 it was shown that theoretically derived C_E values were underestimated in moderate to high wind speeds. This may explain why theoretical mass transfer underestimation of *LE* appeared to be greatest in the early afternoon when highest wind speeds were frequently observed. A potential

explanation for the underestimation of the theoretical C_E values in this study is that the selection of open-water parameterisations for u_* and z_{0m} may not have been appropriate. In McGloin et al. (2014a) it was found that u_* measurements above Logan's Dam were similar to those measured upwind of the reservoir, suggesting that the primary source of turbulence measured above the reservoir was the result of interaction between airflow and land-based terrain. Hence, defining representative u_* and z_{0m} values for small water storages may be problematic because of the complex nature of the airflow and wave formations that exist in such environments. More research is needed in this area.

The constant C_E site specific value found in this study (1.76×10^{-3} for a measurement height of 10 m) is similar to the site-specific values found in Sacks et al. (1994) and Tanny et al. (2008), while it is greater than the values found by Brutsaert (1982) and Rosenberry et al. (2007). In section 3.3 it was found that atmospheric stability played an important role in determining C_E values, where turbulent exchanges of *LE* were promoted during unstable conditions and suppressed during stable conditions. At Logan's Dam the atmosphere immediately above the reservoir tended to be unstable for the majority of the day and night, with short periods of stable conditions in the afternoon when strong winds brought warm dry air over the reservoir surface (for more detailed analysis on diurnal variations in some of the meteorological variables at Logan's Dam see McJannet et al. (2013b) and McGloin et al. (2014b)). This explains why the Tanny et al. (2008) model, which did not account for the influence of atmospheric stability, tended to underestimate *LE* during the morning, evening and night, and overestimate *LE* during the afternoon

An important variable in Granger and Hedstrom's (2011) model is the difference in temperature between the air and water surface. As already discussed, there is evidence to

suggest that unstable conditions promoted turbulent exchanges of *LE* and that stable conditions suppressed exchanges of *LE* at Logan's Dam. However, the importance of stability on *LE* at Logan's Dam does not appear to be as important as results found in Granger and Hedstrom (2011). Granger and Hedstrom (2011) found that the relationship between *LE* and T_s-T_a (R^2=0.20) was stronger than the relationship between *LE* and e_s-e_a (R^2=0.11) at their field site (small lake in northern Canada). This is not the case at Logan's Dam where the relationship between EC *LE* and e_s-e_a (R^2=0.33) is substantially stronger than the relationship with T_s-T_a (negative regression line slope with R^2=0.11).

The Granger and Hedstrom (2011) model may have overestimated the importance of stability and underestimated the significance of e_s-e_a when determining *LE* at Logan's Dam. This was particularly obvious during periods of stable conditions in the early afternoon, when T_s-T_a was negative, e_s-e_a was large and positive and the relationship between EC *LE* measurements and Granger and Hedstrom (2011) estimates was worst. Periods of strongly stable conditions were most frequent during winter, possibly explaining why the relationship between EC *LE* values and Granger and Hedstrom (2011) estimates was so much worse during winter.

The main reason why *LE* estimates from the highly instrumented DYRESM scenario showed a stronger correlation with measured results than estimates from the data limited scenario was due to differences between the over-land and over-water meteorological measurements. Over-land measurements of u and e_a tended to be slightly less than over-water measurements, while over-land measurements of T_a and modelled incident longwave radiation tended to be slightly greater. The higher T_a and longwave radiation values resulted in the greater T_s values predicted by the data limited scenario. However, the overestimates of T_s were counteracted by

the lower u and e_a measurements, resulting in the similar magnitude of the LE values predicted by the two DYRESM scenarios.

In section 3.4 it was shown that DYRESM surface layer temperature results showed very close agreement with $T_{0.1m}$ measurements, but that they were typically greater than T_{skin} estimates. Previous studies have found that a temperature gradient across the molecular boundary layer (top few micrometres of water surface) exists at the air-water interface, such that T_{skin} is systematically cooler (typically by a few tenths of a degree) than the water several centimetres below (Robinson et al., 1984; Wick et al., 1996; Horrocks et al., 2003). Water skin temperature values derived from CNR1 measurements of upwelling long-wave radiation are representative of the temperature of the top few micrometres of the water surface (Donlon et al., 2002). Therefore, it is generally accepted that water surface-atmosphere exchanges can be best described using net radiometer or infrared thermometer measurements of T_{skin} at the air-water interface (Monteith, 1981; Garbe et al., 2007; Minnett et al., 2011), rather than using temperature measurements made just below the interface within the water body itself.

If we assume that T_{skin} values are more representative of the "real" situation at the air-water interface than $T_{0.1m}$ measurements, then the reason for the overestimation of DYRESM estimates of LE for both scenarios becomes clearer, as an overestimation in T_s by DYRESM will also result in an overestimation of LE. The difference in T_{skin} values and DYRESM T_s estimates was particularly evident when the water surface was undergoing substantial cooling via low/negative R_n and positive LE and H values. This explains why DYRESM overestimated LE at night-time, when LE and H were positive and R_n was negative. Best agreement between T_{skin} values and DYRESM T_s estimates was during the late morning/early afternoon, possibly because the strong winds at this time of the day caused mixing of surface

waters (Wick et al., 1996). However, DYRESM still overestimated *LE* during the afternoon. This is most likely because, like the Tanny et al. (2008) mass transfer model, DYRESM did not account for atmospheric stability. Note that DYRESM estimates of *LE* would have been overestimated by more had the fixed C_E value used in DYRESM been the same as the site-specific value found in this study.

If minor improvements are made to the traditional mass transfer and DYRESM models, such as determining representative C_E values and obtaining accurate estimates of T_{skin}, then there is the potential to use these parameterisations in numerical weather prediction systems (such as WRF) to model the effects small lakes have on regional weather. The results of such a study could be important in providing a better understanding of cloud and precipitation processes in areas where small lakes and/or water storages are numerous. Results from the data limited DYRESM scenario are particularly encouraging for *LE* estimation in areas where over-water observations of meteorological data and surface water temperature are not available. The results of studies such as this one could also be used to improve sub-daily estimations of T_s (important implications for water quality and ecology) in hydrological models by using reservoir size and representative C_E values, allowing for more accurate predictions of *LE* (and surface cooling). There is also the potential to use DYRESM to test evaporation reduction measures such as monolayers. DYRESM is independent of any measurements made within the water body and hence is capable of providing an estimate of what evporation would have been if the monolayer was not present, these results could then be compared with direct EC measurements to get an estimate of evaporation reduction.

5. Conclusion

Comparisons between hourly EC *LE* measurements and estimates modelled using a variety of methods were made at a small reservoir in southeast Queensland, Australia. A year of EC *LE* measurements, over-water meteorological measurements, over-land meteorological measurements and water temperature measurements were used in the analysis. Overall, mass transfer estimates of *LE* by the theoretical mass transfer model and the Tanny et al. (2008) and Sacks et al. (1994) models showed the best relationship with measured values under a range of meteorological conditions. The theoretical mass transfer model showed the strongest correlation with measured values, while the Tanny et al. (2008) and Sacks et al. (1994) models had regression equation slopes with the closest proximity to 1. Granger and Hedstrom (2011) model estimates of *LE* showed the worst relationship with measured values, particularly in stable atmospheric conditions when the model appeared to overestimate the impact that stability had on *LE*. The highly instrumented and data limited DYRESM model scenarios performed considerably better than the Granger and Hedstrom (2011) model but worse than the traditional mass transfer models. Both the highly instrumented and data limited DYRESM scenarios tended to overestimate *LE* as a result of overestimating T_s. If minor improvements are made to the traditional mass transfer and DYRESM models then there is the potential to use these parameterisations for many applications, including modelling the effects small lakes have on regional weather.

Acknowledgements

The authors wish to acknowledge the cooperation of Linton and Melinda Brimblecombe who allowed access to the site and installation of equipment. Darren Morrow, Tim Ellis, Rex Keen, Joseph Kemei, Grant Beckett, Glen Ewels, Michael Tobe and Michael Gray provided assistance with the design, installation and maintenance of the equipment. Funding for this research was provided by the Urban Water Security Research Alliance. Furthermore, we want

to thank the Centre for Water Research at the University of Western Australia for providing the model DYRESM and G.L. Irrigation Pty Ltd. who kindly allowed access to survey data for the site.

References

Andreas, E. L. and B. Murphy (1986), Bulk Transfer Coefficients for Heat and Momentum over Leads and Polynyas, *Journal of Physical Oceanography*, 16, 1875-1883. doi:10.1175/1520-0485(1986)016<1875:btcfha>2.0.co;2.

Assouline, S., S. W. Tyler, J. Tanny, S. Cohen, E. Bou-Zeid, M. B. Parlange and G. G. Katul (2008), Evaporation from three water bodies of different sizes and climates: Measurements and scaling analysis, *Advances in Water Resources*, 31, 160-172. doi:10.1016/j.advwatres.2007.07.003.

Balsamo, G., R. Salgado, E. Dutra, S. Boussetta, T. Stockdale and M. Potes (2012), On the contribution of lakes in predicting near-surface temperature in a global weather forecasting model, *Tellus Series a-Dynamic Meteorology and Oceanography*, 64, doi:15829 10.3402/tellusa.v64i0.15829.

Blanken, P. D., W. R. Rouse, A. D. Culf, C. Spence, L. D. Boudreau, J. N. Jasper, B. Kochtubajda, W. M. Schertzer, P. Marsh and D. Verseghy (2000), Eddy covariance measurements of evaporation from Great Slave Lake, Northwest Territories, Canada, *Water Resources Research*, 36, 1069-1077. doi:10.1029/1999WR900338.

Blanken, P. D., W. R. Rouse and W. M. Schertzer (2003), Enhancement of evaporation from a large northern lake by the entrainment of warm, dry air, *Journal of Hydrometeorology*, 4, 680-693.

Bouin, M. N., G. Caniaux, O. Traulle, D. Legain and P. Le Moigne (2012), Long-term heat exchanges over a Mediterranean lagoon, *Journal of Geophysical Research-Atmospheres*, 117, doi:D2310410.1029/2012jd017857.

Brutsaert, W. (1982), *Evaporation into the Atmosphere*, D.Reidel Publishing Company, Dordrecht, Holland.

Bureau of Meteorology (2005), Climate Classification of Australia: Based on a modified Koeppen classification and on a standard 30-year climatology (1961-1990), Canberra, Australia.

Chen, F. and J. Dudhia (2001), Coupling an advanced land surface-hydrology model with the Penn State-NCAR MM5 modeling system. Part I: Model implementation and sensitivity, *Monthly Weather Review*, 129, 569-585. doi:10.1175/1520-0493(2001)129<0569:caalsh>2.0.co;2.

Donlon, C. J., P. J. Minnett, C. Gentemann, T. J. Nightingale, I. J. Barton, B. Ward and M. J. Murray (2002), Toward improved validation of satellite sea surface skin temperature measurements for climate research, *Journal of Climate*, 15, 353-369. doi:10.1175/1520-0442(2002)015<0353:tivoss>2.0.co;2.

Downing, J. A., Y. T. Prairie, J. J. Cole, C. M. Duarte, L. J. Tranvik, R. G. Striegl, W. H. McDowell, P. Kortelainen, N. F. Caraco, J. M. Melack and J. J. Middelburg (2006), The global abundance and size distribution of lakes, ponds, and impoundments, *Limnology and Oceanography*, 51, 2388-2397.

Edson, J. B., A. A. Hinton, K. E. Prada, J. E. Hare and C. W. Fairall (1998), Direct covariance flux estimates from mobile platforms at sea, *Journal of Atmospheric and Oceanic Technology*, 15, 547-562.

Etemad-Shahidi, A., M. Faghihi and J. Imberger (2010), Modelling Thermal Stratification and Artificial De-stratification using DYRESM; Case study: 15-Khordad Reservoir, *International Journal of Environmental Research*, 4, 395-406.

Eugster, W., G. Kling, T. Jonas, J. P. McFadden, A. Wuest, S. MacIntyre and F. S. Chapin (2003), CO2 exchange between air and water in an Arctic Alaskan and midlatitude Swiss lake: Importance of convective mixing, *Journal of Geophysical Research-Atmospheres*, 108, doi:436210.1029/2002jd002653.

Gal, G., J. Imberger, T. Zohary, J. Antenucci, A. Anis and T. Rosenberg (2003), Simulating the thermal dynamics of Lake Kinneret, *Ecological Modelling*, 162, 69-86. doi:10.1016/s0304-3800(02)00380-0.

Garbe, C.S., R.A. Handler and B. Jahne (2007), *Transport at the Air–Sea Interface, Measurements, Models and Parametrizations*, Springer, Berlin, Germany.

Granger, R.J. and N. Hedstrom (2011), Modelling hourly rates of evaporation from small lakes, *Hydrological and Earth System Sciences*, 15, doi:10.5194/hess-15-267-2011.

Horrocks, L. A., B. Candy, T. J. Nightingale, R. W. Saunders, A. O'Carroll and A. R. Harris (2003), Parameterizations of the ocean skin effect and implications for satellite-based measurement of sea-surface temperature, *Journal of Geophysical Research-Oceans*, 108, doi:309610.1029/2002jc001503.

Ikebuchi, S., M. Seki and A. Ohtoh (1988), Evaporation from Lake-Biwa, *Journal of Hydrology*, 102, 427-449. doi:10.1016/0022-1694(88)90110-2.

Imberger, J. and J.C. Patterson (1981), *Dynamic Reservoir Simulation Model - DYRESM: 5*, In: Transport Models for Inland and Coastal Waters. H.B. Fischer (Ed.). Academic Press, New York, 310-361.

Imerito, A. (2010a), *Dynamic Reservoir Simulation Model DYRESM v4: v4.0 Science Manual*, Centre for Water Research University of Western Australia, Perth.

Imerito, A. (2010b), *Dynamic Reservoir Simulation Model DYRESM v4: v4.0 User Guide*, Centre for Water Research University of Western Australia, Perth.

Lee, X, J Finnigan and K Paw U (2005), Coordinate systems and flux bias error, *Handbook of Micrometeorology*, 33-66.

Long, Z., W. Perrie, J. Gyakum, D. Caya and R. Laprise (2007), Northern lake impacts on local seasonal climate, *Journal of Hydrometeorology*, 8, 881-896. doi:10.1175/jhm591.1.

MacKay, M. D., P. J. Neale, C. D. Arp, L. N. D. Domis, X. Fang, G. Gal, K. D. Johnk, G. Kirillin, J. D. Lenters, E. Litchman, S. MacIntyre, P. Marsh, J. Melack, W. M. Mooij, F. Peeters, A. Quesada, S. G. Schladow, M. Schmid, C. Spence and S. L. Stokesr (2009), Modeling lakes and reservoirs in the climate system, *Limnology and Oceanography*, 54, 2315-2329. doi:10.4319/lo.2009.54.6_part_2.2315.

Martynov, A., L. Sushama, R. Laprise, K. Winger and B. Dugas (2012), Interactive lakes in the Canadian Regional Climate Model, version 5: the role of lakes in the regional climate of North America, *Tellus Series a-Dynamic Meteorology and Oceanography*, 64, doi:16226 10.3402/tellusa.v64i0.16226.

Massman, W. J. (2000), A simple method for estimating frequency response corrections for eddy covariance systems, *Agricultural and Forest Meteorology*, 104, 185-198. doi:10.1016/SO168-1923(00)00164-7.

McGloin, R., H. McGowan, D. McJannet, F. Cook, A. Sogachev and S. Burn (2014a), Quantification of surface energy fluxes from a small water body using scintillometry and eddy covariance, *Water Resources Research*, 50, 494-513. doi:10.1002/2013wr013899.

McGloin, R., McGowan, H. and McJannet, D. (2014b), Effects of diurnal, intra-seasonal and seasonal climate variability on the energy balance of a small subtropical reservoir, *Int. J. Climatol*. Advance online publication. 494-513. doi: 10.1002/joc.4147.

McJannet, D. L., F. J. Cook and S. Burn (2013a), Comparison of techniques for estimating evaporation from an irrigation water storage, *Water Resources Research*, doi:10.1002/wrcr.20125.

McJannet, D.L., F.J. Cook, R.P. McGloin, H. A. McGowan and S. Burn (2011), Estimation of evaporation and sensible heat flux from open water using a large aperture scintillometer, *Water Resources Research*, 47, 1-14. doi:10.1029/2010WR010155.

McJannet, D.L., F.J. Cook, R.P. McGloin, H. A. McGowan, S. Burn and B. S. Sherman (2013b), Long-term energy flux measurements over an irrigation water storage using scintillometry *Agricultural and Forest Meteorology*, 168, 93-107. doi:10.1016/j.agrformet.2012.08.013.

Minnett, P. J., M. Smith and B. Ward (2011), Measurements of the oceanic thermal skin effect, *Deep-Sea Research Part Ii-Topical Studies in Oceanography*, 58, 861-868. doi:10.1016/j.dsr2.2010.10.024.

Mironov, D., L. Rontu, E. Kourzeneva and A. Terzhevik (2010), Towards improved representation of lakes in numerical weather prediction and climate models: Introduction to the special issue of Boreal Environment Research, *Boreal Environment Research*, 15, 97-99.

Monteith, J. L. (1965), *The State and Movement of Water in Living Organisims: Evaporation and the Environment*, Cambridge Univ. Press, London.

Monteith, J. L. (1981), Evaporation and Surface Temperature, *Quarterly Journal of the Royal Meteorological Society*, 107, 1-27. doi:10.1256/smsqj.45101.

Nordbo, A., S. Launiainen, I. Mammarella, M. Lepparanta, J. Huotari, A. Ojala and T. Vesala (2011), Long-term energy flux measurements and energy balance over a small boreal lake using eddy covariance technique, *Journal of Geophysical Research-Atmospheres*, 116, 1-17. doi:D02119 10.1029/2010jd014542.

Paulson, C. A. (1970), The Mathematical Representation of Wind Speed and Temperature Profiles in the Unstable Atmospheric Surface Layer, *Journal of Applied Meteorology*, 9, 857-861.

Perroud, M., S. Goyette, A. Martynov, M. Beniston and O. Anneville (2009), Simulation of multiannual thermal profiles in deep Lake Geneva: A comparison of one-dimensional lake models, *Limnology and Oceanography*, 54, 1574-1594. doi:10.4319/lo.2009.54.5.1574.

Pielke, R. A. (2001), Influence of the spatial distribution of vegetation and soils on the prediction of cumulus convective rainfall, *Reviews of Geophysics*, 39, 151-177. doi:10.1029/1999rg000072.

Pitman, A. J. (2003), The evolution of, and revolution in, land surface schemes designed for climate models, *International Journal of Climatology*, 23, 479-510. doi:10.1002/joc.893.

Priestly, C.H.B. and R.J. Taylor (1972), On the Assessment of Surface Heat Flux and Evaporation using Large-scale Parameters, *Monthly Weather Review*, 100, 81-92. doi:10.1175/1520-0493(1972)100<0081:otaosh>2.3.co;2.

Robinson, I. S., N. C. Wells and H. Charnock (1984), The sea surface thermal boundary layer and its relevance to the measurement of sea surface temperature by airborne and spaceborne radiometers, *International Journal of Remote Sensing*, 5, 19-45.

Rosenberry, D. O., T. C. Winter, D. C. Buso and G. E. Likens (2007), Comparison of 15 evaporation methods applied to a small mountain lake in the northeastern USA, *Journal of Hydrology*, 340, 149-166. doi:10.1016/j.jhydrol.2007.03.018.

Rouse, W. R., C. J. Oswald, J. Binyamin, C. R. Spence, W. M. Schertzer, P. D. Blanken, N. Bussieres and C. R. Duguay (2005), The role of northern lakes in a regional energy balance, *Journal of Hydrometeorology*, 6, 291-305. doi:10.1175/jhm421.1.

Sacks, L.A., T.M. Lee and M.J. Radell (1994), Comparison of energy-budget evaporation losses from two morphometrically different Florida seepage lakes, *Journal of Hydrology*, 156, 311-334.

Sene, K. J., J. H. C. Gash and D. D. McNeil (1991), Evaporation from a Tropical lake: Comparison of theory with direct measurements, *Journal of Hydrology*, 127, 193-217. doi:10.1016/0022-1694(93)90208-Q.

Sridhar, V. and R. L. Elliott (2002), On the development of a simple downwelling longwave radiation scheme, *Agricultural and Forest Meteorology*, 112, 237-243. doi:10.1016/s0168-1923(02)00129-6.

Stull, R.B. (1988), *An Introduction to Boundary Layer Meteorology*, Kluwer Academic Publishers, Netherlands.

Tanny, J., S. Cohen, S. Assouline, F. Lange, A. Grava, D. Berger, B. Teltch and M. B. Parlange (2008), Evaporation from a small water reservoir: Direct measurements and estimates, *Journal of Hydrology*, 351, 218-229. doi:10.1016/j.jhydrol.2007.12.012.

Tanny, J., S. Cohen, D. Berger, B. Teltch, Y. Mekhmandarov, M. Bahar, G. Katul and S. Assouline (2011), Evaporation from a reservoir with fluctuating water level: Correcting for limited fetch, *Journal of Hydrology*, 404, 146-156. doi:10.1016/j.jhydrol.2011.04.025.

Webb, E. K., G. I. Pearman and R. Leuning (1980), Correction of flux measurements for density effects due to heat and water vapour transfer, *Quarterly Journal of the Royal Meteorological Society*, 106, 85-100. doi:10.1002/qj.49710644707.

Weinberger, S. and M. Vetter (2012), Using the hydrodynamic model DYRESM based on results of a regional climate model to estimate water temperature changes at Lake Ammersee, *Ecological Modelling*, 244, 38-48. doi:10.1016/j.ecolmodel.2012.06.016.

Wick, G. A., W. J. Emery, L. H. Kantha and P. Schlussel (1996), The behavior of the bulk-skin sea surface temperature difference under varying wind speed and heat flux, *Journal of Physical Oceanography*, 26, 1969-1988. doi:10.1175/1520-0485(1996)026<1969:tbotbs>2.0.co;2.

Wiebe, A., A. P. Sturman and H. A. McGowan (2011), Wavelet Analysis of Atmospheric Turbulence over a Coral Reef Flat, *Journal of Atmospheric and Oceanic Technology.*, 28, 698-708. doi:10.1175/2010JTECHA1485.1.

Zilitinkevich, S. (1969), On the computation of the basic parameters of the interaction between the atmosphere and the ocean, *Tellus* 21, 17-24.

Figure 1: Relationship between hourly EC *LE* measurements and values modelled using a) the theoretical mass transfer model and b) the Tanny et al. (2008) mass transfer model. The solid lines indicate the regression equations and the dashed lines represent the 1:1 lines.

Figure 2: a) Diurnal and b) seasonal variation in the difference between mean modelled and measured *LE* values. Note that only the best performing method from Table 1 is included (i.e. Tanny et al. (2008)). The data presented consists of the difference between mean modelled and measured *LE* values during specific 3-hour time blocks and each season. Mean *LE* values were calculated using hourly measurements/predictions from the entire measurement period (note that for fair comparison averages were constructed using data that was restricted to periods when hourly *LE* values from EC and each modelling technique were available). The mean EC *LE* values for each time block/season are also included at the bottom of each figure.

Figure 3: Theoretical C_E values against wind speed and values derived using the empirical wind function ($C_E=1.5\times10^{-3}+1.6\times10^{-3}/u$).

Figure 4: Diurnal variation in mean $T_{0.1m}$, T_{skin} and DYRESM estimates of T_s. Averages consist of the mean temperature values during 3-hour time blocks and were calculated using hourly temperature measurements/predictions from the entire measurement period.

(a)

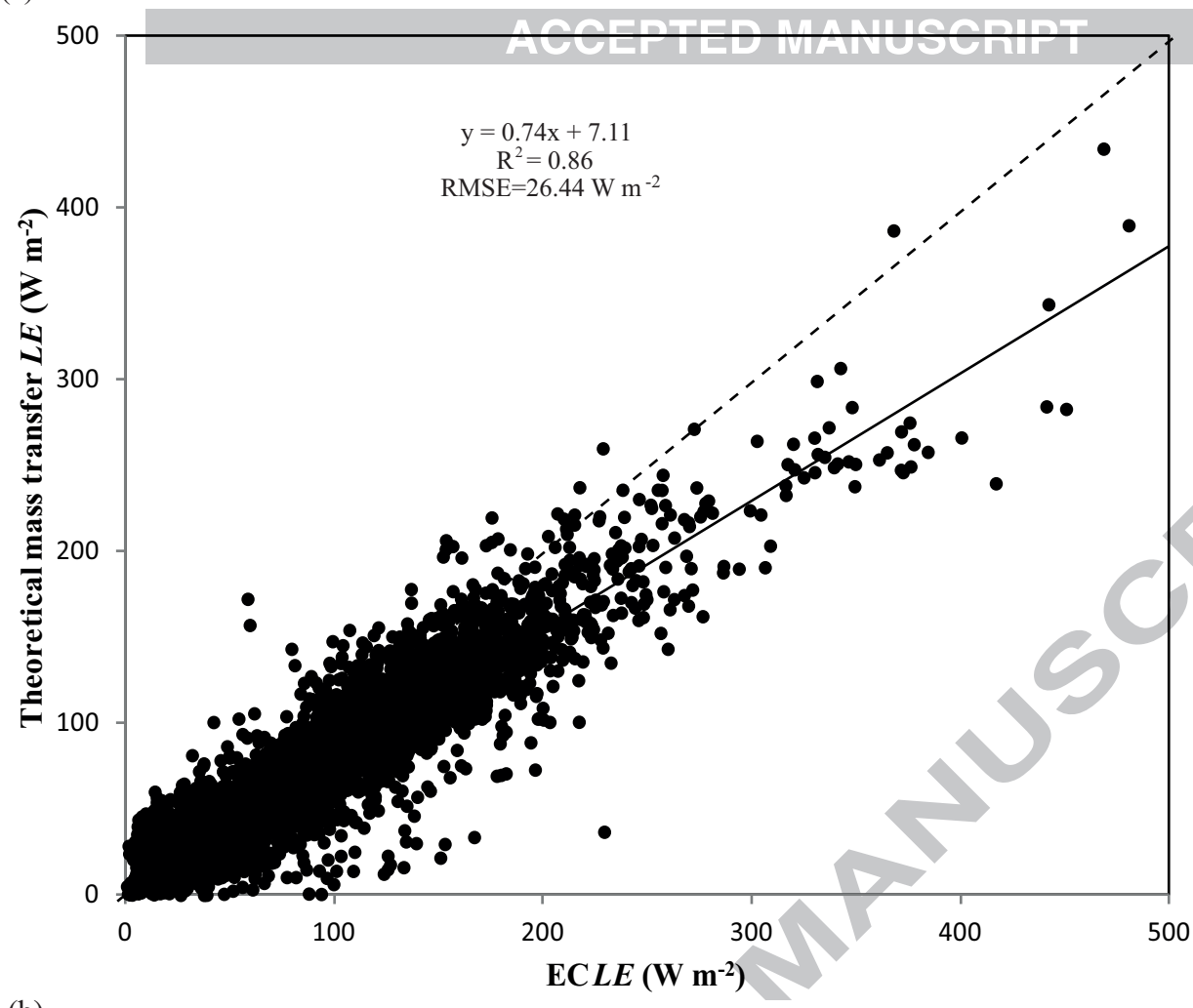

(b)

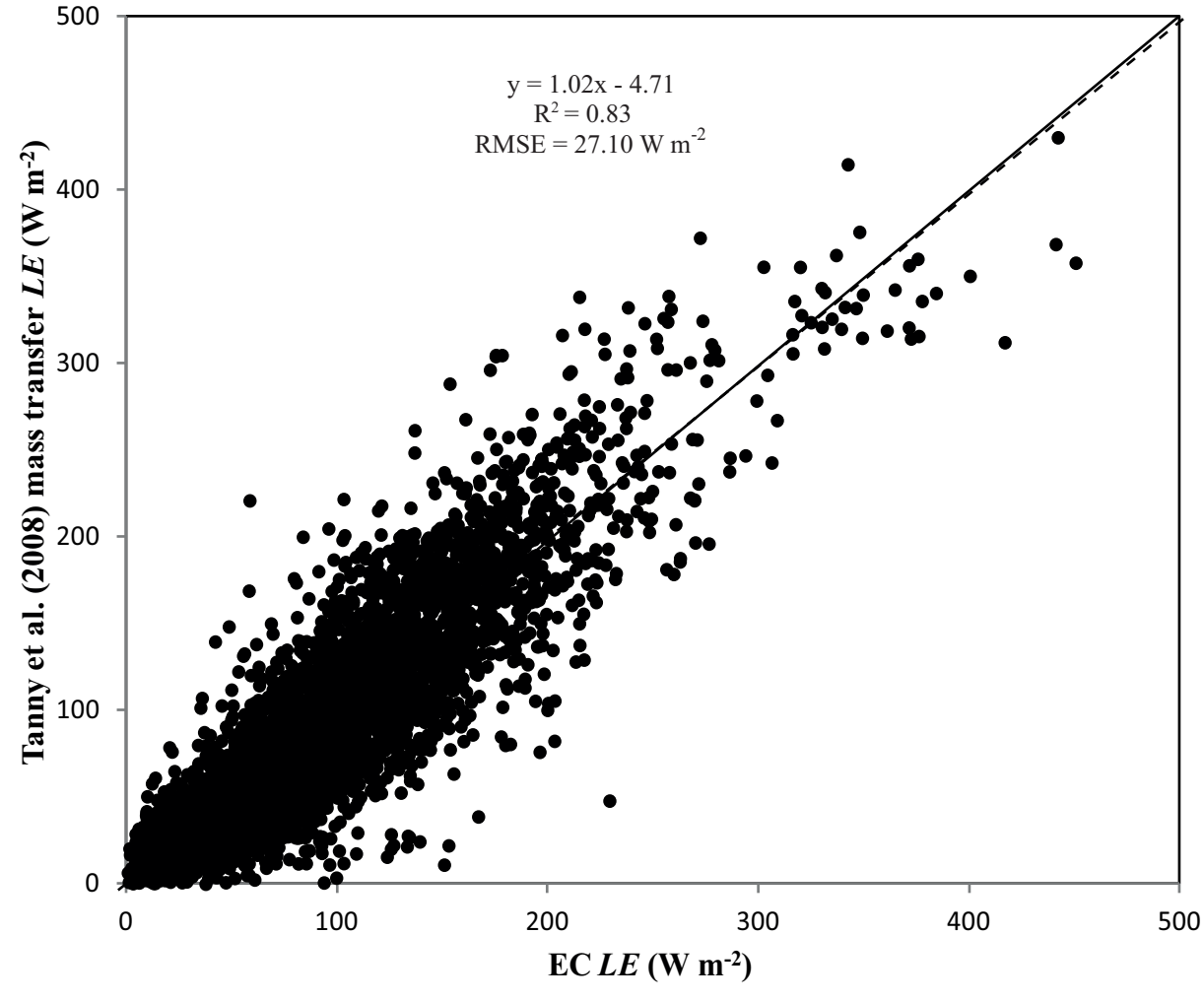

a)

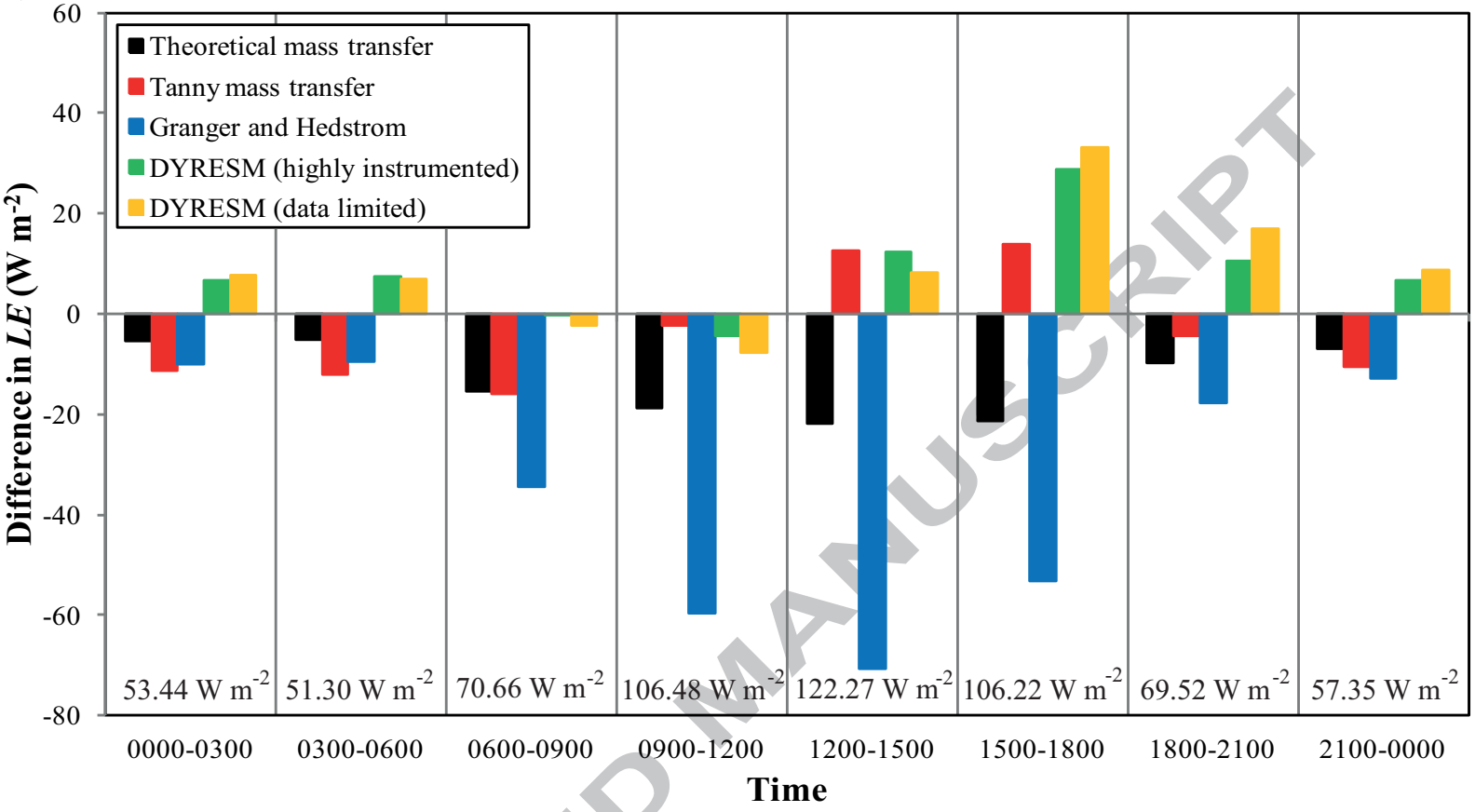

b)

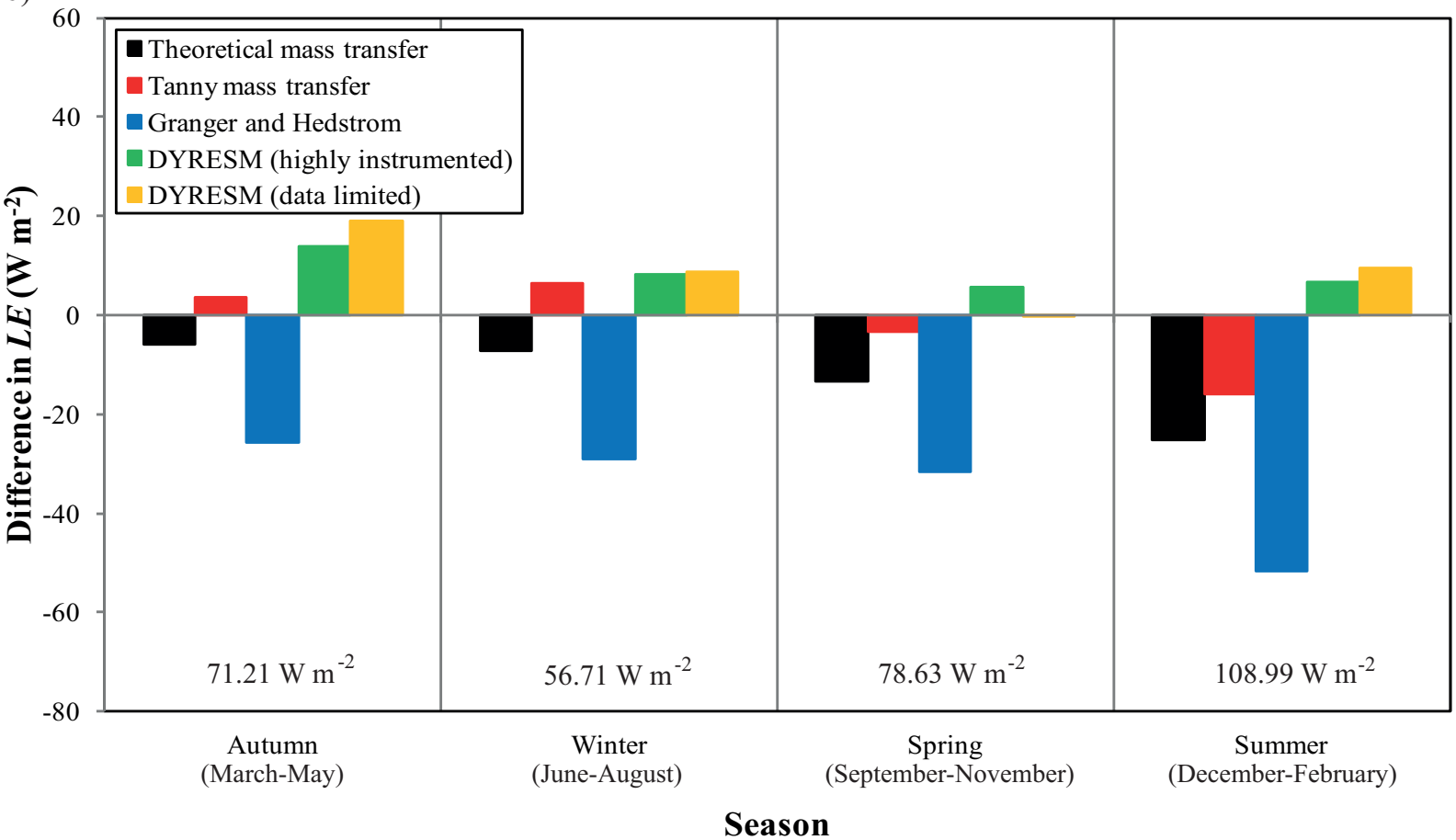

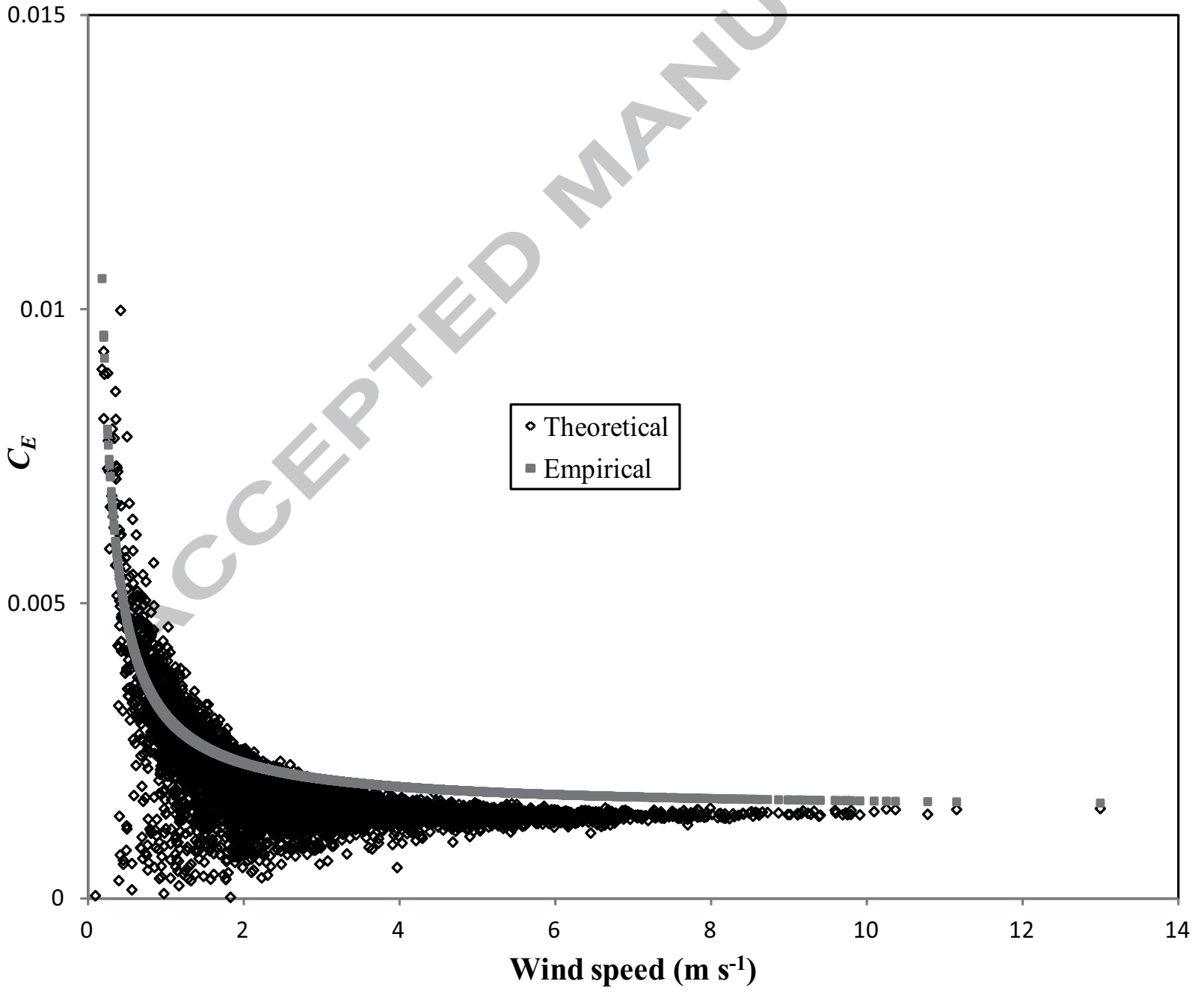

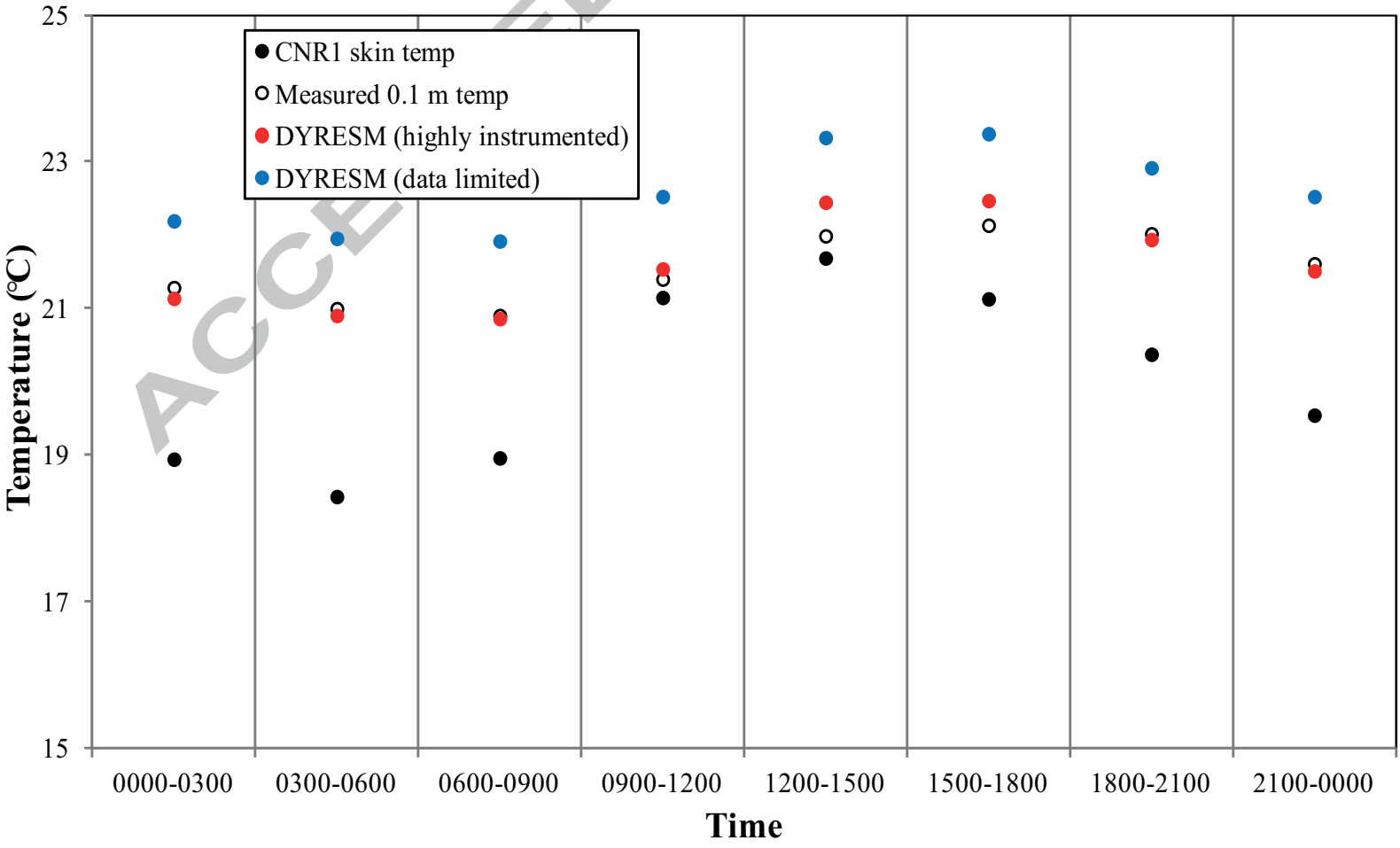

Highlights

- Various modelling techniques were used to estimate sub-daily latent heat fluxes.
- The field site was a small reservoir in southeast Queensland, Australia.
- The theoretical mass transfer model was the best performing model in this study.
- The Granger and Hedstrom model performed the worst.
- Estimates by the DYRESM model tended to be greater than measured values.